J. Membrane Biol. 199, 15–28 (2004)
DOI: 10.1007/s00232-004-0672-0

The Journal of
Membrane
Biology

Steady-State Interactions of Glibenclamide with CFTR: Evidence for Multiple Sites in the Pore

Z.-R. Zhang*, **S.** Zeltwanger*, **N.A.** McCarty
School of Biology, Georgia Institute of Technology, and Department of Physiology, Emory University School of Medicine, Atlanta, GA 30332, USA

Received: 26 December 2003/Revised: 9 March 2004

Abstract. The objective of the present study was to clarify the mechanism by which the sulfonylurea drug, glibenclamide, inhibits single CFTR channels in excised patches from *Xenopus* oocytes. Glibenclamide blocks the open pore of the channel via binding at multiple sites with varying kinetics. In the absence of glibenclamide, open-channel bursts exhibited a flickery intraburst closed state (C1); this is due to block of the pore by the pH buffer, TES. Application of 25 μM glibenclamide to the cytoplasmic solution resulted in the appearance of two drug-induced intraburst closed states (C2, C3) of widely different duration, which differed in pH-dependence. The kinetics of interaction with the C3 state, but not the C2 state, were strongly voltage-dependent. The durations of both the C2 and C3 states were concentration-dependent, indicating a non-linear reaction scheme. Application of drug also increased the burst duration, which is consistent with an open-channel blocking mechanism. A kinetic model is proposed. These results indicate that glibenclamide interacts with open CFTR channels in a complex manner, involving interactions with multiple binding sites in the channel pore.

Key words: Cystic fibrosis transmembrane conductance regulator — Chloride channel — Open channel blocker — Permeation — Sulfonylurea

Introduction

The cystic fibrosis transmembrane conductance regulator (CFTR) is a member of the ATP-binding cassette (ABC) superfamily and functions as a Cl^- channel regulated by protein kinase A (PKA) (Riordan et al., 1989; Anderson et al., 1991; Bear et al., 1992). The predicted structure of CFTR includes two membrane-spanning domains (MSDs) each composed of six membrane-spanning segments, two nucleotide-binding domains (NBD1 and NBD2), and a regulatory (R) domain. Several pharmacological agents have been shown to inhibit CFTR Cl^- currents through pore blockade (reviewed in McCarty, 2000; Dawson et al., 2003). These include members of the arylaminobenzoates such as diphenylamine-2-carboxylate (DPC), flufenamic acid (FFA), and 5-nitro-2-(3-phenylpropylamino)-benzoate (NPPB) (McCarty et al., 1993; Zhang, Zeltwanger & McCarty, 2000; Walsh, Long & Shen, 1999), and members of the sulfonylureas (Schultz et al., 1996; Sheppard & Robinson, 1997), the most potent of which is glibenclamide (Mehnert & Karg, 1969). Glibenclamide has been shown to modulate other members of the ABC superfamily, including the sulfonylurea receptor, which forms the regulatory subunit of ATP-dependent K^+ channels (Aguilar-Bryan et al., 1995) and P-glycoprotein (Golstein et al., 1999). Glibenclamide also modulates other channels, such as ATP-sensitive K^+ channels (Sturgess et al., 1985), renal K^+ channels (ROMK2) (McNicholas et al., 1996), swelling-activated and Ca^{2+} -activated Cl^- channels (Yamazaki & Hume, 1997), and outwardly rectifying Cl^- channels (Rabe, Disser & Fromter, 1995; Julien et al., 1999). However, many of these modulatory effects are thought to be indirect, with glibenclamide conferring its effects through members of the ABC superfamily associated with these channels (Schwiebert et al., 1999). Since glibenclamide sensitivity appears to be a common feature of ABC transporters, identification of the glibenclamide binding site(s) in CFTR may hold promise for identification of the binding sites in other ABC superfamily members.

Although several reports have shown that glibenclamide inhibits CFTR channel activity, the exact

Correspondence to: N.A. McCarty; email: nael.mccarty@biology.gatech.edu

*These authors contributed equally to this work

mechanism of inhibition has remained unclear. Sheppard and Welsh (1992) were the first to show that glibenclamide inhibits whole-cell CFTR Cl^- currents in a dose-dependent manner when the drug was applied to the extracellular bath. They reported this inhibition to be relatively voltage-independent and poorly reversible. However, this compound has also been shown to inhibit PKA (Okuno et al., 1988), which makes mechanistic interpretations of inhibition of CFTR whole-cell currents unclear. Later studies using single-channel measurements demonstrated that application of glibenclamide to the cytoplasmic face of excised patches containing wild-type CFTR channels resulted in a dose-dependent, reversible decrease in open probability (P_O) (Schultz et al., 1996; Sheppard & Robinson, 1997). However, the effects of glibenclamide on interburst and intraburst kinetics were not consistent in these studies. One complicating factor in these previous studies was the use of patches containing more than one active channel.

The primary objective of this study was to clarify the mechanism of glibenclamide inhibition of CFTR and to develop a quantitative model to describe its action. We used kinetic analysis of single-channel currents from patches expressing low numbers of CFTR channels, where distinction between interburst closed periods and intraburst blocked periods is clearer. Under these conditions, we were able to identify multiple classes of blocked states, each likely representing different sites of glibenclamide interaction with CFTR.

Materials and Methods

Oocyte Preparation and cRNA Injection

The methods used are similar to those described previously (McCarty et al., 1993; McDonough et al., 1994; Zeltwanger, Zhang & McCarty, 2000). Briefly, stage V–VI *Xenopus* oocytes were prepared as previously described (Quick et al., 1992) and were incubated at 18°C in a modified Liebovitz's L-15 medium with addition of HEPES (pH 7.5), gentamicin, penicillin, and streptomycin. cRNA was prepared from a construct carrying the full coding region of wild-type (*wt*) CFTR in the pAlter vector (Promega; Madison, WI). Oocytes were injected with 5 ng of CFTR cRNA plus 0.6 ng of cRNA for the human β-2 adrenergic receptor (β2-AR), which allows activation of PKA-regulated currents by addition of isoproterenol to the bath. Recordings were made 42 to 96 hours after cRNA injection.

Electrophysiology

All single-channel studies were performed on excised, inside-out patches. Oocytes were shrunk in a hypertonic solution (in mM: 200 potassium aspartate, 20 KCl, 1 $MgCl_2$, 10 EGTA, and 10 HEPES-KOH, pH 7.2) and the oocyte vitelline membrane was then removed. Pipettes were pulled from borosilicate glass (Sutter Instrument Co.; Novato, CA), and had an average resistance of ~10 MΩ when filled with standard pipette solution (in mM: 150 NMDG-Cl, 5 $MgCl_2$, and 10 TES, adjusted with Tris to pH 7.4). Some experiments used a low-Cl^- pipette solution (in mM: 5 NMDG-Cl, 5 $MgCl_2$, 135 NMDG-aspartate, and 10 TES, adjusted with Tris to pH 7.4); these experiments were corrected for junction potentials as described (Zhang et al., 2002). Prior to recording, oocytes were placed in a bath solution containing (in mM): 96 NaCl, 2 KCl, 1 $MgCl_2$, 5 HEPES, adjusted with NaOH to pH 7.5. Seal resistances were in the range of 200 GΩ . In most experiments the presence of CFTR in the patch was tested by application of 1–5 μM isoproterenol to the bath solution prior to excision. After excision, the chamber was perfused with intracellular solution (in mM: 150 NMDG-Cl, 1.1 $MgCl_2$, 2 Tris-EGTA, 1 MgATP, 2–10 TES, pH adjusted to 6.3 or 7.3 with Tris). CFTR was activated by addition of 50 U/mL PKA (Promega). Channel currents were measured at room temperature (~22°C) with an AI2120 amplifier or an Axopatch 200B amplifier (Axon Instruments, Inc.; Foster City, CA), and were recorded at 10 kHz on DAT tape (Sony, model DTC-790). Data were subsequently played back and filtered with a 4-pole Bessel filter (Warner Instruments; Hamden, CT) either at 100 Hz (for burst analysis) or 1 kHz (for intraburst kinetic studies) and acquired by the computer at 2 ms/point (burst analysis) or 100 μs/point (intraburst kinetic studies), using the Fetchex program of pCLAMP (Axon).

Kinetic Analysis

In experiments using the inside-out configuration, channels were first activated with isoproterenol in cell-attached mode. Rundown was observed in some patches immediately after excision; this likely reflects dephosphorylation of the R-domain by membrane-associated protein phosphatases (Zhu et al., 1999), since 1 mM ATP was continuously present. This rundown affected only interburst behavior, not intraburst behavior (Luo et al., 1998). After application of PKA, activity levels were fairly constant in a given patch over several minutes (Zhang et al., 2002). For kinetic analysis of gating, all recordings were performed after the initial rundown, and only recordings with minimal rundown were selected. Time-dependent rundown of CFTR channels had no apparent effect on intraburst kinetics. To standardize conditions, all patches were exposed to PKA throughout the recording. Data in the presence of blocker were obtained under the same conditions as the control data. Due to the high acquisition rate used for analysis, necessary in order to capture brief events, recordings analyzed were typically ~45 s in duration; each recording included multiple bursts.

Kinetic Analysis of Interburst Gating

Dwell-time analysis of open bursts was performed using Igor software (Igor Pro, version 3.14; Wavemetrics; Lake Oswego, OR). Open bursts in the presence and absence of blockers were defined as intervals separated by closings of 1 s or greater. A shorter interburst discriminator (80 ms) has been used in previous studies in the absence of blocker (Zhang et al., 2000); in this study, the long duration of glibenclamide-induced closed state C3 (*see below*) required the use of a longer interburst discriminator in order to distinguish between ATP-dependent gating closures and intraburst blockade. Furthermore, patches containing only a single open level were used in the analysis of bursts in the presence or absence of blocker. After measuring the burst duration, the events were sorted from shortest to longest and plotted against the cumulative probability that a particular burst would last at least time (t). Fitting of these distributions provided mean burst durations in each condition.

Analysis of Intraburst Blockade Kinetics

A 50% threshold criterion was used to distinguish transitions between open and closed/blocked current levels. The probability density functions (pdf) of the intraburst open and closed time distributions were generated from pooled events in each patch. As described below, two glibenclamide-induced closed times (τ_{C2} and τ_{C3}) were resolved. Because the frequency of the longer intraburst closure (C3) is very low, it could not be accurately estimated using a traditional pdf. To study the kinetics of these events, dwell-time analysis was performed on closings within a burst that were longer than 10 ms (roughly five-fold longer than τ_{C2}). All-points histograms were made with Igor software, and then fit to a Gaussian function. The intraburst open probability (P_O) was then determined using the following equation:

$P_O = A_O/(A_O + A_C)$, where A_O and A_C are the areas in the amplitude histogram contributed by the open and closed states, respectively.

Statistics

All reported values are presented as mean ± SEM, unless otherwise noted. Statistical analysis was performed employing the *t*-test for paired or unpaired measurements (Sigma-Stat, Jandel Scientific; San Rafael, CA) as appropriate for each set of experiments, with $P \leq 0.05$ considered indicative of significance.

Source of Reagents

Unless otherwise noted, all reagents were obtained from Sigma (St. Louis, MO). DPC (N-phenylanthranilic acid) was from Aldrich (Milwaukee, WI); L-15 media was from Gibco/BRL (Gaithersburg, MD). Glibenclamide and DPC were prepared as stock solutions in DMSO at 100 mM. At the dilutions used, DMSO was without effect on CFTR currents (*not shown*).

Results

Effects of Glibenclamide on Intraburst Kinetics: Evidence for Multiple Binding Sites

Figure 1 shows the effect of glibenclamide on the fine structure of open bursts of phosphorylated *wt*-CFTR channels at cytosolic pH 7.3 over increasing time resolutions. In the presence of 25 μM glibenclamide, the period within an open burst contains multiple distributions of blockade events, some lasting for only ms (Fig. 1*A*, *lower panel*), and some lasting for tens of ms (Fig. 1*A*, *middle panel*). Also evident at the highest time resolution are very brief transitions to the closed current level, lasting <1 ms in duration. These very brief transitions were also observed in the absence of glibenclamide (Fig. 2*A*); the apparent frequency of these very brief blocked states (C1) was sensitive to both cytoplasmic pH and to the concentration of TES used in these solutions. When [TES] was reduced from 10 mM to 2 mM, the apparent single-channel conductance increased ~20% due to relief from fast flickery block (Fig. 3). The duration of the short, TES-induced blocked state in the absence of glibenclamide (τ_{C1}) was

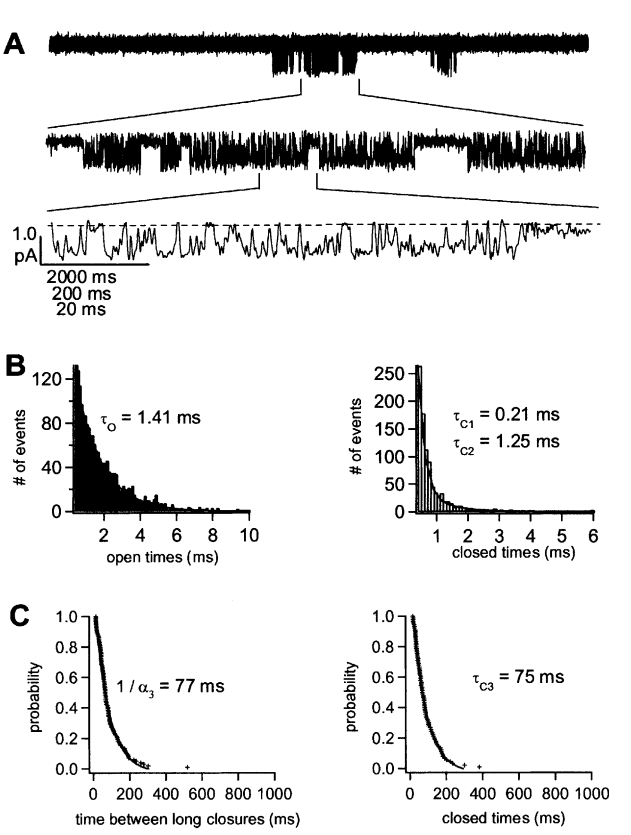

Fig. 1. Effect of glibenclamide on intraburst kinetics of CFTR at pH 7.3. (*A*) CFTR channels in the presence of 25 μM glibenclamide exhibit distinct populations of intraburst closings that can be observed when the burst is viewed at multiple levels of resolution (10 s, *top*; 1 s, *middle*; 100 ms, *bottom*). Short, flickery closures and two longer closed states that are not present in the absence of blocker, but found in the presence of glibenclamide, are shown in the *bottom* (intermediate closed state) and *middle* (long closed state) panels. The recording shown is a segment from a record lasting 45 s at $V_M = -100$ mV, filtered at 1 kHz, which included 16 bursts. (*B*) Two dwell-time probability density functions (pdfs) constructed from 4878 intraburst openings and closings from the patch shown in (*A*). (*C*) Cumulative dwell-time analysis of the long blocking state (*right*) and time between long blocking events (*left*) from the patch shown in (*A*). Closed-and open-time constants shown are for this patch only; mean values are summarized in Table 1. The dashed line represents the closed state for the 100 ms trace.

not significantly different at pH 7.3 compared to at pH 6.3 (τ_{C1} = 0.24 and 0.23 ms, respectively; Table 1), and was similar to the value of 0.27 ms reported previously (McCarty et al., 1993). (It should be noted that τ_{C1} is likely to be an inaccurate estimation of the actual duration of this very brief state because this value is below the resolution of our acquisition parameters [Colquhoun & Sigworth, 1995].) Hence, the flickery intraburst blocked events observed in our records both in the presence and absence of glibenclamide reflect block of the pore by the pH buffer, TES, used in our intracellular solutions. Previous single-channel studies of CFTR and other chloride channels have shown that even in the absence of

Table 1. Effects of blockers on mean intraburst time constants, at $V_M = -100$ mV

pH	Condition	τ_O	τ_{C1} or τ_{C1*}	τ_{C2}	τ_{C3}	n
7.3	No blocker	4.95 ± 0.58	0.24 ± 0.01	–	–	29
	5 μM Glibenclamide	4.3 ± 0.27[a]	0.22 ± 0.03	–	18.2 ± 2.15[a]	6
	25 μM Glibenclamide	1.47 ± 0.20[b]	0.25 ± 0.03	1.96 ± 0.39	37.8 ± 7.37	12
	100 μM Glibenclamide	1.27 ± 0.22[b]	0.32 ± 0.04	3.33 ± 0.66[a]	73.0 ± 6.23[a]	5
	100 μM DPC	1.29 ± 0.25[b]	0.44 ± 0.02[b]	–	–	3
	25 μM Glibenclamide + 100 μM DPC	1.25 ± 0.16[b,c]	0.30 ± 0.02	1.53 ± 0.36	44.7 ± 5.03[b,c]	10
6.3	No blocker	8.04 ± 1.29[d]	0.23 ± 0.01	–	–	8
	25 μM Glibenclamide (5)	3.54 ± 1.65[b,d]	0.23 ± 0.01	2.13 ± 0.86	38.8 ± 5.27	5

All values are reported in ms; n = number of patches, each with multiple bursts.
[a] $P \leq 0.05$ compared to 25 μM glibenclamide at the same pH.
[b] $P \leq 0.05$ compared to no blocker at the same pH.
[c] $P \leq 0.05$ compared to 25 μM glibenclamide alone in paired experiments at the same pH.
[d] $P \leq 0.05$ compared to the same conditions at pH 7.3.

exogenous blockers, open-channel bursts exhibit a flickery intraburst component in excised patches (Hanrahan & Tabcharani, 1990; Haws et al., 1992; McCarty et al., 1993; Winter et al., 1994; Ishihara & Welsh, 1997; Mathews et al., 1998) which arises from the use of sulfonic acid-derivatized buffers such as MOPS, HEPES, and TES in the intracellular recording solution. However, as the interactions between glibenclamide and the pore are pH-dependent (*see below*), it was necessary to include TES at a concentration of 10 mM in subsequent experiments in order to maintain control over solution pH.

Figure 1*B* shows the closed-level dwell-time pdf constructed from the brief intraburst blocked events (≤ 10 ms in duration) for a representative patch in the presence of 25 μM glibenclamide. In contrast to pdfs for channels in the absence of glibenclamide, fitting the pdfs in the presence of glibenclamide required a double-exponential function, revealing two closed-time constants (Fig. 1*B*) that reflect the introduction of the C2 blocked state with mean duration $\tau_{C2} = 1.96 \pm 0.39$ ms. To quantify the duration of the longest intraburst blocking events (τ_{C3}), dwell-time analysis was performed on intraburst transitions to the closed current level lasting at least 10 ms. This cutoff, over five-fold the mean value for τ_{C2}, was used in order to prevent contamination from the briefer blocking events. These long blocked-state events were then used to construct a cumulative dwell-time histogram for each patch (Fig. 1*C*, right panel). Exponential fitting of the cumulative dwell-time histograms for these longest blocking events yielded a mean τ_{C3} of 37.8 ± 7.37 ms at pH 7.3.

Because there are three different intraburst closed states in the presence of drug, we use the terms short, intermediate, and long to describe the events that have respective time constants τ_{C1}, τ_{C2}, and τ_{C3}. Thus, C1 refers to the brief flicker observed even in the absence of glibenclamide, while C2 and C3 are new glibenclamide-induced blocked states observed only in the presence of glibenclamide. With 25 μM glibenclamide, the short closed state predominated, with τ_{C1} comprising 95 ± 1% ($n = 12$) of the area beneath the fit for brief events at pH 7.3. The intermediate, glibenclamide-induced intraburst closed state (C2) occurred less frequently, comprising only 5 ± 1% (Table 1, $n = 12$) of the area beneath the fit for brief events. The long blocking event (C3) occurred much less frequently than the faster events (*see* Fig. 1*A*; middle panel).

In the presence of 25 μM drug, τ_{C1} was not significantly different from the value obtained in the absence of drug (Table 1), suggesting that this state is not drug-induced (but see below). At this concentration, the C2 and C3 states were easily distinguished, as τ_{C3} was approximately twenty-fold longer than τ_{C2}. At a lower concentration (5 μM), transitions to the C2 state were not observed and the duration of the C3 state was reduced (Table 1). Alternatively, the C3 state may have been eliminated and the duration of the C2 state prolonged. With 100 μM glibenclamide, transitions to both the C2 and C3 states were observed; the durations of both τ_{C2} and τ_{C3} were increased compared to those in the presence of 25 μM glibenclamide. Hence, the closed dwell-time durations for the C2 and C3 states were dependent upon drug concentration, which is not predicted from a simple linear reaction scheme. This observation suggests that transitions directly between the C2 and C3 states are possible (*see* Fig. 9*A*). In contrast, the duration of τ_{C1} was not obviously sensitive to drug concentration.

Analysis of intraburst open times revealed a significant decrease in open-time in the presence of drug (Fig. 1*B*) when compared to unblocked channels at the same pH (Fig. 2*B*). In the presence of 25 μM glibenclamide at pH 7.3, $\tau_O = 1.47 \pm 0.20$ ms (Table 1), representing an approximately three-fold decrease from the τ_O in the absence of blocker. The reduction of open time by glibenclamide exhibited a

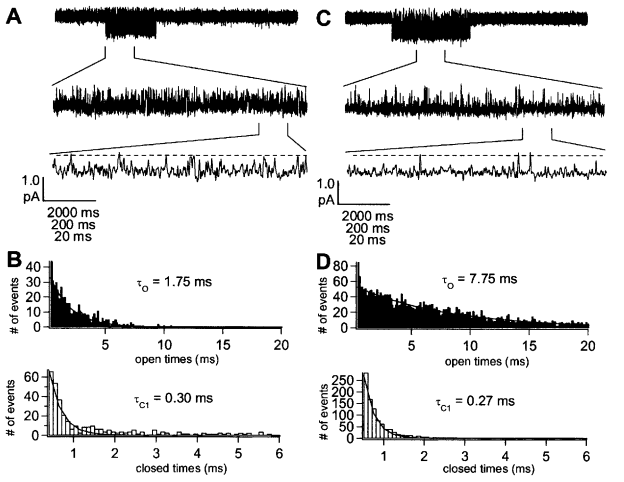

Fig. 2. Intraburst kinetics of unblocked CFTR channels at pH 7.3 and 6.3. (*A*) At pH 7.3, a brief, flickery closure can be observed within a burst when the burst is viewed at multiple levels of resolution. $V_M = -100$ mV; recording filtered at 1 kHz. (*B*) Two pdfs constructed from 760 intraburst openings and closings at pH 7.3 from the patch shown in (*A*). (*C*) At pH 6.3 in the absence of glibenclamide, the brief flickery closure occurs less frequently than at pH 7.3. (*D*) The pdf constructed from 4451 intraburst openings and closings at pH 6.3 from the patch shown in (*C*). Closed- and open-time constants shown are for these patches only; mean values are summarized in Table 1. The dashed lines denote the closed state for the 100 ms stretches.

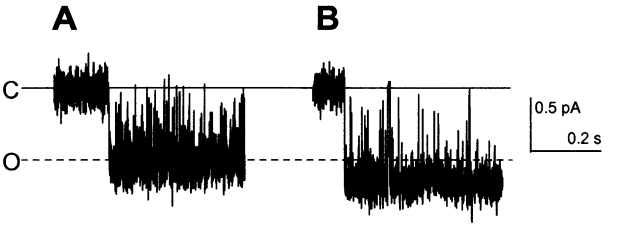

Fig. 3. Nature of the fast flicker in the absence of glibenclamide. Two records (550 ms each) from a single patch in the presence of (*A*) 10 mM or (*B*) 2 mM TES as the pH buffer for the intracellular solution. The frequency of the fast flicker is related to the concentration of buffer. With low [TES], the apparent single-channel conductance is increased, due to relief from fast flickery block. Solid line represents closed channel current level; dashed line represents open-channel current level for the record with 10 mM TES.

nonlinear relationship with drug concentration between 0 and 100 μM (Fig. 4, Table 1), consistent with the presence of multiple binding sites.

To estimate the apparent forward-rate (α_1) to the C1 state we used the data at 0 μM and 25 μM glibenclamide (for which n are greatest) and the following equation:

$$\alpha_1 = \frac{(1/\tau_O) \times A}{100}$$

where τ_O is the intraburst open time in the absence or presence of glibenclamide and A is the percent of the area beneath the closed durations curve fit (for events ≤ 10 ms only), which is due to the brief closed-time constant (τ_{C1}). Interestingly, the data indicated an increased frequency of the brief flickers in the presence of glibenclamide (Table 2), although their apparent duration was unchanged (Table 1). The apparent increase in α_1 upon addition of glibenclamide suggests that some component of the fast flicker in the presence of drug may actually reflect a very fast component of block by glibenclamide, which is of approximately the same duration as the blocked state arising from TES; however, the increase in α_1 was not large enough to reduce apparent single-channel conductance. Similar results were shown previously for block of the CFTR pore by DPC, in which case the brief interaction between drug and channel increases the frequency of fast flicker without introduction of a new well-defined closed state (McCarty et al., 1993). Alternatively, the presence of the negatively-charged glibenclamide may simply enhance the on-rate of the negatively-charged unprotonated TES molecule to its binding site. To differentiate between brief events that are observed in the presence and absence of glibenclamide, we use hereafter the terms C1* and τ_{C1}* indicate the brief closed state, and its duration, in the presence of glibenclamide.

Using Eq. 1 in a similar manner we also estimated $\alpha_2 = 1.39 \times 10^6\ M^{-1}\ s^{-1}$ (Table 2). This results in a binding rate of 34.7 s^{-1} in the presence of 25 μM glibenclamide, which correlates relatively well with the observed frequency of the intermediate closed state evident upon visual inspection of the traces (Fig. 1*A*; bottom panel). The off-rate (β2) of glibenclamide from site C2 was determined as $1/\tau_{C2} = \beta_2 = 510 \pm 100\ s^{-1}$. Similarly, to assess the apparent on-rate (α_3) of the blocker to the C3 state, an events list was constructed from all of the open durations between intraburst closures longer than 10 ms, using data with 25 μM glibenclamide (Fig. 1 *C*, left). Exponential fitting of these dwell-time histograms yielded time constants, the inverse of which represents the on-rate (α_3). We estimated α_3 to be $0.62 \pm 0.10 \times 10^6\ M^{-1}\ s^{-1}$. The off-rate ($\beta_3$) from the site responsible for the C3 state was determined as $1/\tau_{C3} = \beta_3 = 26.5 \pm 5\ s^{-1}$. Because the actual on-rate α_1 cannot be determined, since we do not know the concentration of the blocking species responsible for the C1 events, the dissociation constant for interactions at this site cannot be estimated with confidence. From α_2 and β_2, the dissociation constant (K_{d2}) of glibenclamide from the site representing the C2 state was estimated as: $K_{d2} = \beta_2/\alpha_2 \cong 367$ μM. Similarly, from α_3 and β_3 we estimated the dissociation constant of glibenclamide from this site (K_{d3}) as: $K_{d3} = \beta_3/\alpha_3 \cong 43$ μM. Because the off-rates are concentration-dependent, it should be noted that these dissociation constants are relevant only at a glibenclamide concentration of 25 μM. Furthermore,

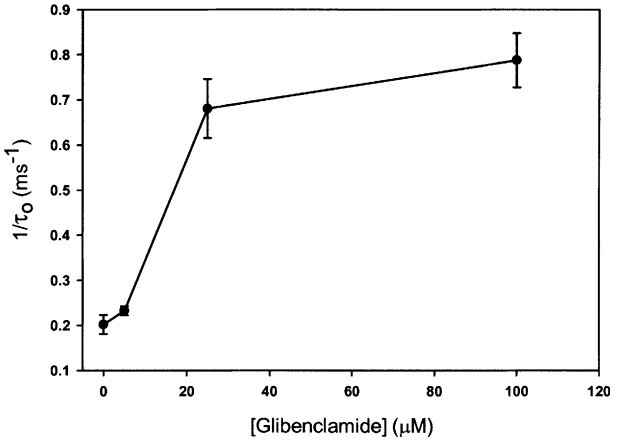

Fig. 4. Concentration dependence of block. Inverse of open time is plotted as a function of concentration for experiments with 0 μM (n = 29), 5 μM (n = 6), 25 μM (n = 12), and 100 μM (n = 5) glibenclamide (mean ± SEM). The non-linear relationship suggests that direct transitions between blocked states (C2 and C3) are possible.

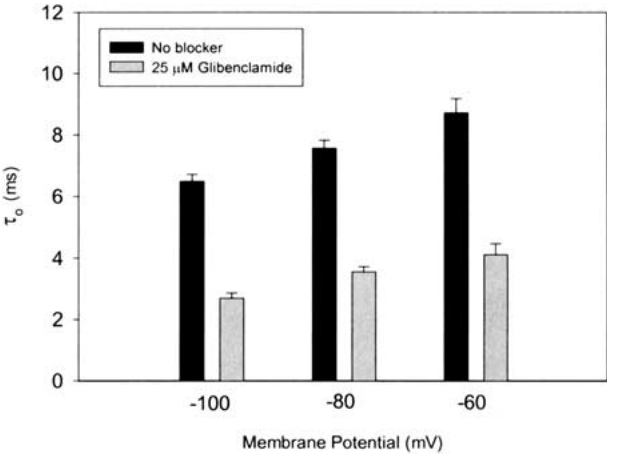

Fig. 5. Voltage dependence of open dwell-time, in the absence of blocker (*black bars*) and in the presence of 25 μM glibenclamide (*gray bars*) (mean ± SEM; n = 6–7 at each potential).

block of macroscopic CFTR currents by glibenclamide is typically found to have a K_d in the range of 100 μM. In our excised patch experiments with 25 μM cytoplasmic glibenclamide, the interactions with the C2 and C3 sites give K_d values that were lower (for C2) and higher (for C3). Hence, the microscopic blocking events described here reasonably predict the block of macroscopic currents. We also point out that our K_d estimates relate only to the effects of glibenclamide on intraburst behavior; glibenclamide may also affect gating of CFTR (Zeltwanger et al., 2000; Cui & McCarty, 2003), which would result in a secondary impact on overall P_o by affecting both intra- and interburst states.

Thus, the application of glibenclamide to the cytoplasmic side of CFTR channels introduced intraburst closed or blocked states (C2 and C3) not observed in the absence of blocker, and an increase in the rapid flicker that may reflect a third glibenclamide-induced closed state (C1*). These effects of glibenclamide on open channels can be explained by proposing multiple binding sites. These effects of glibenclamide were fully reversible upon washout of the drug; reversibility of block by glibenclamide has been shown previously (Zhou, Hu & Hwang, 2002).

Dependence of Intraburst Kinetics on pH

Sheppard and Robinson (1997) previously reported that lowering the pH of the cytoplasmic bath in the presence of glibenclamide decreased the drug-induced inhibition of P_O. The mechanism for this attenuated inhibition at acidic pH was proposed to be a decrease in prevalence of the anionic form of glibenclamide. However, the pH dependence of microscopic on- and off-rates was not examined. To investigate the effects of glibenclamide on the open state of CFTR, the intraburst kinetics were examined at cytosolic pH 6.3 and compared to those at pH 7.3. Reduction of pH from 7.3 to 6.3 had no apparent effect on channel gating.

Similar to the data at pH 7.3, the τ_O for channels studied at pH 6.3 was also decreased approximately two-fold by the addition of 25 μM glibenclamide to the cytosolic bath. The durations of the C1, C2, and C3 states (and therefore the reverse rate constants) were not pH-dependent (Table 1, Table 2). The apparent glibenclamide-induced increase in $\alpha 1$ at pH 6.3 was similar to that at pH 7.3. However, the forward binding rates α_2 and α_3 were decreased by 45% and 77% at cytosolic pH 6.3, respectively, compared to those rates at pH 7.3 (Table 2). Therefore, the calculated dissociation constants K_{d2} and K_{d3} were increased to 617 and 184 μM respectively, representing a >2-fold decrease in apparent affinity. The pKa for glibenclamide is ~6.3 (Sheppard & Robinson, 1997). Shifting cytosolic pH from 7.3 to 6.3 would be expected to cause a 45% reduction in the concentration of charged drug (Zhang et al., 2000), which should equally affect α_2 and α_3 . Therefore, the 45% reduction in α_2 at pH 6.3 only reflects the change in concentration of the charged species. In contrast, the greater effect of low pH on α_3 suggests that pH has direct effects on affinity at the site corresponding to the C3 state. These data show that glibenclamide can bind to a lower-affinity site (represented by the C2 state), which is not pH-dependent, as well as to a higher-affinity site (represented by the C3 state), which has an apparent pH dependency.

Voltage Dependence of Block

Cytoplasmic glibenclamide blocks CFTR channels only at hyperpolarizing potentials (*see* Fig. 7).

Table 2. Effects of blockers on mean intraburst rate constants, at $V_m = -100$ mV

pH	Condition	α_1 (s^{-1})	α_2 (M^{-1} s^{-1})	α_3 (M^{-1} s^{-1})	β_1 (s^{-1})	β_2 (s^{-1})	β_3 (s^{-1})	*n*
7.3	No blocker	260 ± 21	–	–	4343 ± 160	–	–	29
	25 μM Glibenclamide	793 ± 132[a]	1.39 ± 0.28 × 10^6	0.62 ± 0.10 × 10^6	4000 ± 480	510 ± 100	27 ± 5	12
	100 μM DPC	843 ± 184[a]	–	–	2341 ± 130[a]	–	–	3
	25 μM Glibenclamide + 100 μM DPC	820 ± 92[a]	1.52 ± 0.32 × 10^6	0.70 ± 0.10 × 10^6	3300 ± 220	650 ± 150	22 ± 2[b]	10
6.3	No blocker	146 ± 21	–	–	4432 ± 244	–	–	8
	25 μM Glibenclamide	1117 ± 540[a]	0.76 ± 0.38 × 10^{6c}	0.14 ± 0.04 × 10^{6c}	4310 ± 113	470 ± 150	26 ± 4	5

The on-rates of flickery block due to the pH buffer (α_1) are given in units of s^{-1} since the concentration of the charged blocking species is unknown.
[a] $P \leq 0.05$ compared to no blocker at the same pH.
[b] $P \leq 0.05$ compared to 25 μM glibenclamide at the same pH in paired experiments.
[c] $P \leq 0.05$ compared to the same conditions at pH 7.3.
n = number of patches, each with multiple bursts.

Table 3. Voltage dependence of microscopic kinetics

Voltage mV	Condition	τ_O ms	τ_{Cl} or τ_{Cl*} ms	τ_{C2} ms	τ_{C3} ms	α_3 $M^{-1}s^{-1}$	*m2*	*n*
−100	No blocker	6.49 ± 0.23	0.29 ± 0.02					6
	Glibenclamide, 25 μM	2.70 ± 0.17[a]	0.26 ± 0.02	1.56 ± 0.32	35.1 ± 1.80	0.63 ± 0.04 × 10^6	0.09 ± 0.03	6
−80	No blocker	7.57 ± 0.26	0.25 ± 0.01					7
	Glibenclamide, 25 μM	3.56 ± 0.17[a,b]	0.21 ± 0.04	1.34 ± 0.17	21.3 ± 1.90[b]	0.48 ± 0.03 × 10^{6b}	0.05 ± 0.01	6
−60	No blocker	8.72 ± 0.46	0.23 ± 0.01					7
	Glibenclamide, 25 μM	4.12 ± 0.35[a,b]	0.19 ± 0.02	0.99 ± 0.05	11.8 ± 0.50[b]	0.31 ± 0.05 × 10^{6b}	0.06 ± 0.01	6

[a] $P \leq 0.05$ compared to no blocker.
[b] $P \leq 0.05$ compared to −100 mV.
m2: the fractional contribution of the C2 state to the population of brief events (≤10 ms); *n* = number of patches, each with multiple bursts.

Although voltage-dependent reduction of P_O in CFTR by glibenclamide has been shown by other investigators, the effects of membrane potential on the microscopic kinetics of interaction between drug and binding site(s) have been reported only for long blocking events (Zhou et al., 2002). Hence, in a separate set of experiments we measured the kinetics of interaction at −100, −80, and −60 mV (Table 3). In the absence of exogenous blocker, open-time decreased with increasing hyperpolarization (Fig. 5), partly due to voltage-dependent block by TES (Zhou et al., 2001; Cai, Scott-Ward & Sheppard, 2003). In the presence of 25 μM glibenclamide, open times were reduced at each potential, but there was not an obvious change in the voltage dependence of τ_O. This is likely due to the fact that the apparent on-rate of TES to its binding site is considerably greater than the on-rate of glibenclamide to each of its sites (Table 2; Fig. 1). The duration of neither the TES-induced C1 state nor the glibenclamide-induced C1* state were strongly voltage-dependent (Table 3). Neither the forward nor reverse rates of interaction with the C2 state were voltage-dependent; τ_{C2} changed from 0.99 to 1.56 ms between −60 and −100 mV, respectively ($P = 0.147$; Fig. 6, Table 3): The fraction of brief closures due to glibenclamide (m2 in Table 3) also did not shift, indicating that neither α_1 nor α_2 are voltage-dependent over this voltage range. In contrast, both the duration of the C3 state and the forward rate constant to this state were strongly voltage-dependent (Fig. 6, Table 3). As the membrane potential was hyperpolarized from −60 to −100 mV, τ_{C3} increased 3-fold ($P < 0.001$) and the apparent forward reaction rate (α_3) doubled ($P = 0.009$). Hence, the voltage-dependence of glibenclamide-induced inhibition of CFTR arises predominantly from the voltage dependence of interaction with the site characterized by high affinity and slow kinetics, representing the C3 state.

Effect of Glibenclamide on Burst Kinetics

The effects of glibenclamide on burst duration are unclear; some investigators reported an increase in burst duration upon exposure to glibenclamide (Sheppard & Robinson, 1997), while others reported a decrease (Schultz et al., 1996). In our experiments, the block induced by glibenclamide at hyperpolarizing potentials, but not at depolarizing potentials, was associated with an increase in burst duration (Fig. 7). To quantify the effects of glibenclamide on burst duration, dwell-time analysis of widely-separated

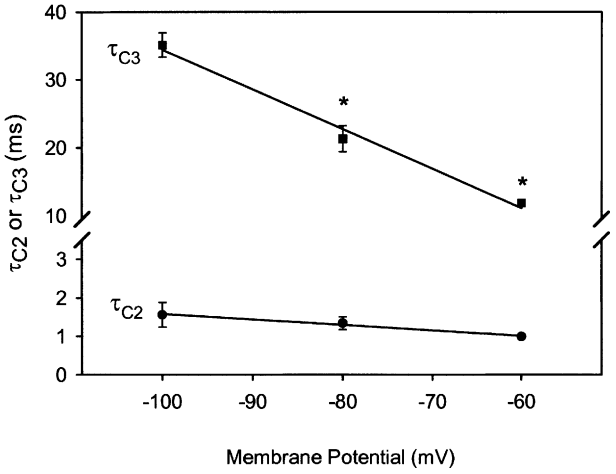

Fig. 6. Voltage dependence of closed dwell-times for the C2 and C3 states (mean ± SEM; $n = 6$ at each potential). Asterisks indicate significant difference from the value at $V_M = -100$ mV.

bursts from multiple patches containing a single open level was performed at various membrane potentials, in the absence and presence of the blocker. The cumulative dwell-time histograms at each potential were fit best with single-exponential functions, providing the mean open burst durations in the absence and presence of glibenclamide (Fig. 7*C*). In the absence of glibenclamide, mean open burst duration was 3030 ± 433 ms at −100 mV. Addition of 25 μM glibenclamide to the cytoplasmic side of the patch resulted in an increase in mean burst duration to 4348 ± 629 ms at −100 mV ($P = 0.033$). This increase in the duration of the bursting state in the presence of glibenclamide is consistent with previous findings (Sheppard & Robinson, 1997), and suggests that one mechanism by which glibenclamide inhibits CFTR is via open channel block (*see* Neher & Steinbach, 1978; Colquhoun & Hawkes, 1995). The effect of glibenclamide on burst duration was more prominent as the membrane potential was hyperpolarized, consistent with increased flickery block at these potentials (Fig. 7*C*).

The C2 and C3 States Represent Glibenclamide Binding in the Pore

Sheppard and Robinson (1997) first suggested that glibenclamide binds within the pore of CFTR. Two observations confirm that the sites underlying both the C2 and C3 states reside in the channel pore. First, neither of the intraburst closed states was evident at positive membrane potentials (Fig. 7), indicating that each state represents voltage-dependent interactions of the drug with sites lying within the electrical field. Second, the microscopic kinetics of interaction with both pore sites were affected by a ten-fold reduction in pipette Cl^- concentration. With pipette [Cl^-] at 15 mM and 25 μM glibenclamide on the cytoplasmic side, τ_{C2} and τ_{C3} were increased to 28.0 ± 3.0 and 184.2 ± 22.1 ms, respectively ($P < 0.001$, $n = 4$). In contrast, τ_{C1} and τ_{C1}* with reduced pipette [Cl^-] were nearly identical (0.35 ± 0.01 and 0.38 ± 0.02 ms, respectively). These data show that the off-rates of glibenclamide from at least the C2 and C3 pore sites are strongly sensitive to the driving force for Cl^-. As the driving force for Cl^- exit at −100 mV was increased ten-fold, the off-rates from both the C2 and C3 sites decreased > 5-fold. Strong hyperpolarization may deplete Cl^- binding at a site within the external aspect of the pore, diminishing electrostatic repulsion between Cl^- and glibenclamide, resulting in stabilization of glibenclamide at its binding site(s) (Zhou et al., 2002). These data are consistent with the notion that the binding sites for both the C2 and C3 intraburst closed states are localized within the pore, and may reside near a chloride binding site or sites.

DPC and Glibenclamide Interact within the Pore of CFTR

The foregoing evidence suggests that the pore of CFTR contains two well-defined binding sites for glibenclamide, and that the kinetics of binding at these two sites are rather slow compared to the kinetics of binding for other CFTR blockers, such as the arylaminobenzoate, DPC. Previous studies have provided evidence that DPC acts as an open-channel blocker of CFTR by interaction with a single binding site (McCarty et al., 1993; McDonough et al., 1994; Zhang et al., 2000). Portions of the DPC binding site have been identified (McDonough et al., 1994). As a step toward identifying the binding sites for glibenclamide, we determined whether these two blockers can interact within the pore. Before examining the kinetics of channel activity in the presence of both blockers, we determined the kinetics in the presence of DPC alone. In agreement with previous studies it was found that DPC blocks CFTR on a single-channel level by increasing both the frequency and duration of flickery closures within an open burst at hyperpolarizing potentials (McCarty et al., 1993; McDonough et al., 1994), leading to a decrease in τ_O. Unlike channels in the presence of glibenclamide, only one homogeneously-distributed population of intraburst closed states was observed in the presence of DPC. Consistent with previous results, we found that pdfs constructed from the intraburst closures in the presence of DPC revealed no new closed states, but only a slight rightward shift in the histogram. Fitting multiple closed-time pdfs with a single-exponential function resulted in a mean intraburst closed-time constant (τ_{C1}) of 0.44 ± 0.02 ms (Table 1) in the presence of DPC.

In the presence of glibenclamide, the addition of DPC altered intraburst blocking kinetics. Time

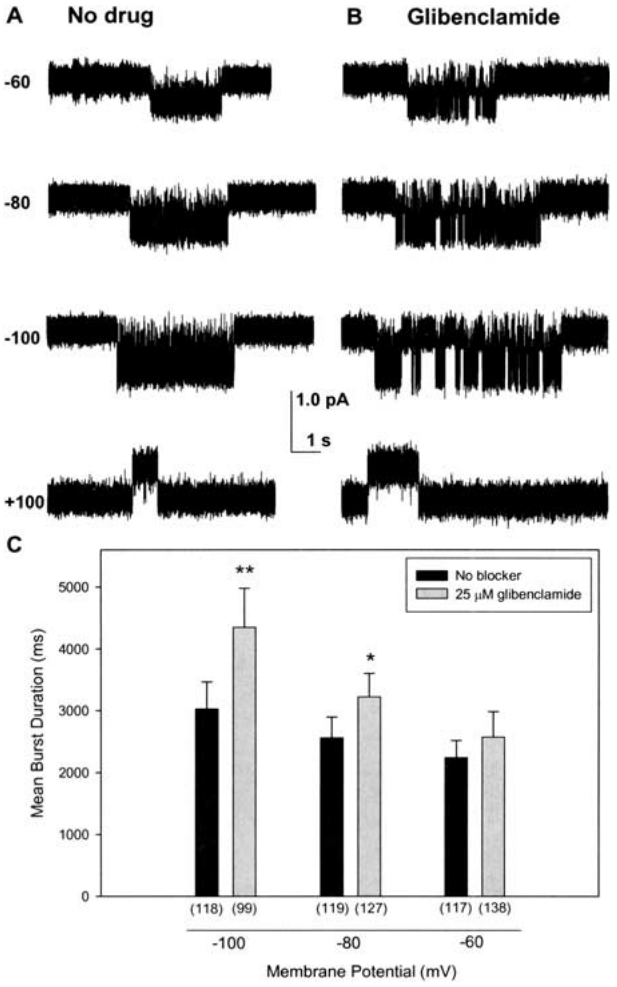

Fig. 7. Glibenclamide induces flickery block and lengthens open bursts. (*A*) Single CFTR bursts at various membrane potentials (as noted at the left of the figure, in mV) in the absence of glibenclamide. Openings are downward with negative potentials, and upward with positive potentials. (*B*) Single bursts in the presence of 25 μM glibenclamide at the same potentials. (*C*) Summary of the effect of glibenclamide on burst duration, at each voltage (*$P = 0.047$; **$P = 0.033$). Only isolated bursts to a single open level were used for this analysis. The number of bursts for each condition are shown in parentheses. All traces shown were filtered at 1 kHz.

constants for all three glibenclamide-induced closed states (τ_{C1}*, τ_{C2}, and τ_{C3}), as well as the open state (τ_O, were calculated using the same methods that were used to calculate the time constants in the presence of glibenclamide alone; τ_O was decreased to 1.25 ± 0.16 ms in the presence of 100 μM DPC and 25 μM glibenclamide. While τ_O varied from patch to patch, in paired experiments addition of 100 μM DPC to the intracellular solution containing 25 μM glibenclamide consistently resulted in a decrease in τ_O in each experiment (Fig. 8*A*). The average DPC-induced decrease in τ_O in the presence of glibenclamide was 34 ± 7% ($P < 0.05$). This result is consistent with an increase in the blocking rate due to an increase in the overall concentration of blocker. While τ_{C1}* and τ_{C2} were not significantly different in the presence of DPC and glibenclamide, compared to in the presence of glibenclamide alone (Table 1), τ_{C3} was increased by concurrent application of DPC, consistent with an effect of DPC on stabilization of the interaction of glibenclamide with the binding site responsible for the C3 state. In paired experiments, addition of DPC to a glibenclamide-containing intracellular solution increased τ_{C3} in every patch by an average of 101 ± 22% (Fig. 8*B*). Hence, DPC appeared to retard the unbinding of glibenclamide from the C3 site (increased τ_{C3}), while having no effect on the rate of binding to this site (α_3 was unchanged; Table 2). These results are consistent with the notion that the pore (or inner vestibule) of CFTR is large, as first suggested by Linsdell (Linsdell & Hanrahan, 1996), since both glibenclamide and DPC (as well as chloride and water) could be accommodated simultaneously. Zhou and coworkers have also suggested that glibenclamide and isethionate could simultaneously occupy the pore (Zhou et al., 2002).

Discussion

The kinetic analysis presented here demonstrates that glibenclamide interacts with CFTR in a complex manner that includes binding to at least two sites that lead to intraburst block. While block of CFTR Cl^- currents by glibenclamide has been known for a decade, the detailed kinetics of interaction between CFTR and glibenclamide have been investigated only recently (Zhou et al., 2002). That study suggested that glibenclamide interacts with CFTR channels in a simple manner, resulting in the appearance of a single class of drug-induced blocked states. In contrast, our results suggest a multifaceted mechanism of inhibition that involves clearly defined intermediate and long blocked states within an open burst.

Glibenclamide Inhibits by an Open-Channel Mechanism

The effect of glibenclamide on burst duration is controversial. In the absence of exogenous blockers the distinction between brief intraburst closures and longer-lived closed states representing termination of the ATP-dependent gating cycle is clear, if channel number is low. However, this distinction becomes vaguer in the presence of glibenclamide, which appears to reside in the pore much longer than other open-channel blockers of CFTR, and particularly when patches include multiple active channels. To distinguish between long glibenclamide-induced blockade events and the termination of a burst one should examine the kinetics when the channel activity

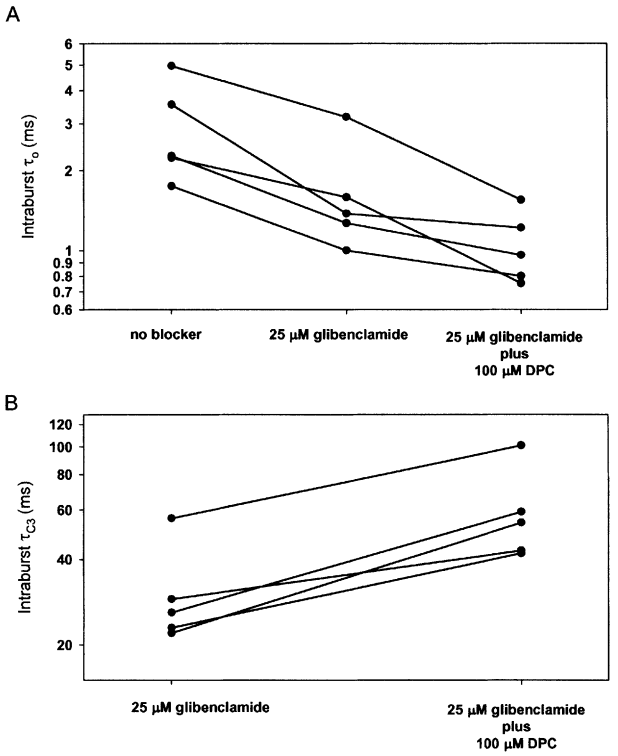

Fig. 8. Effects of DPC on blockade by glibenclamide in five paired experiments. (*A*) τ_O in the absence of drugs and in the presence of either 25 μM glibenclamide or 25 μM glibenclamide plus 100 μM DPC. (*B*) τ_{C3} in the presence of either 25 μM glibenclamide or 25 μM glibenclamide plus 100 μM DPC.

is relatively low in order to obtain long interburst durations and clearly defined openings (Zeltwanger et al., 1999). This is critical for accurate assessment of the effects of glibenclamide on CFTR channel activity. For example, both of the early single-channel studies on effects of glibenclamide (Schultz et al., 1996; Sheppard & Robinson, 1997) reported interburst durations < 150 ms and overall $P_O > 0.35$ in the unblocked state. Although an overall decrease in P_O in the presence of glibenclamide is apparent in both studies, differentiation of gating closures from blocking events is impossible under these conditions given the long duration of the C3 state reported here. Schultz and coworkers (Schultz et al., 1996) reported a decrease in the burst duration after addition of glibenclamide, while Sheppard and Robinson (1997) reported an increase in burst duration with glibenclamide. Both studies reported a decrease in the interburst duration (between openings) after addition of glibenclamide. This is likely due to misinterpretation of some of the glibenclamide-induced intraburst blocking events as real gating closures, which would lead to an overestimation of the opening rate (inverse of interburst duration) of the channel. The record shown in Fig. 1*A* exhibits long intraburst drug-induced closed durations that could easily be misinterpreted as channel closures; in our study, we avoided this error by only studying patches that had very low activity.

Our analysis of clearly isolated bursts results in an obvious distinction between glibenclamide-induced intraburst closures and the much longer gating closures. In our experiments, burst duration was clearly increased in the presence of 25 μM glibenclamide; this effect was enhanced by hyperpolarization (Fig. 7). The increase in burst duration in the presence of glibenclamide confirms that this drug inhibits CFTR, at least in part, by an open-channel block mechanism. A recent study by Hwang and coworkers (Zhou et al., 2002) used the opposite approach in relying upon the K1250A-CFTR mutant that exhibits greatly diminished (but not completely abolished) ATP-dependent gating. In that study, bursts were not identifiable, so no effect of glibenclamide on burst duration could be investigated.

The Effects of Glibenclamide on Intraburst Kinetics: Evidence for Multiple Sites of Action

As described above, the kinetic mechanism underlying the glibenclamide-induced decline in single-channel P_O reported in previous studies remains unclear. We studied the effects of glibenclamide on open CFTR channels by examining the intraburst blocking events within clearly defined bursts. Even in the absence of blocker, a flickery intraburst behavior is commonly observed in both cell-attached and excised patches from cells expressing CFTR (McCarty et al., 1993; Fischer & Machen, 1994; Zhou, Hu & Hwang, 2001). In excised patches they arise from block of the pore by the pH buffer; in our experiments, this is TES. We show here a pH dependence of the on-rate of this brief flickery closure, which would be expected from titration of the charged species of TES. This is important to note when assessing the pH dependence of the on-rate of glibenclamide. Because τ_O does not equal the burst duration even in the absence of glibenclamide, the rate of the background flicker should be subtracted from the overall blocking rate ($1/\tau_O$) in the presence of exogenous blocker in order to accurately calculate the true on-rate of blocker (*see* Ogden & Colquhoun, 1985; Colquhoun & Hawkes, 1995).

The appearance of multiple drug-induced closed states upon addition of glibenclamide to the cytoplasmic side of excised patches is indicative of multiple sites of action in the CFTR protein. The C2 and C3 drug-induced closed states represent interaction of glibenclamide with two sites that lie within the permeation pathway, as indicated by the dependence of τ_{C2} and τ_{C3} upon the permeant anion concentration. The site corresponding to the C2 state does not appear to lie deep within the pore (far from the cytoplasmic end of the pore) because the kinetics of

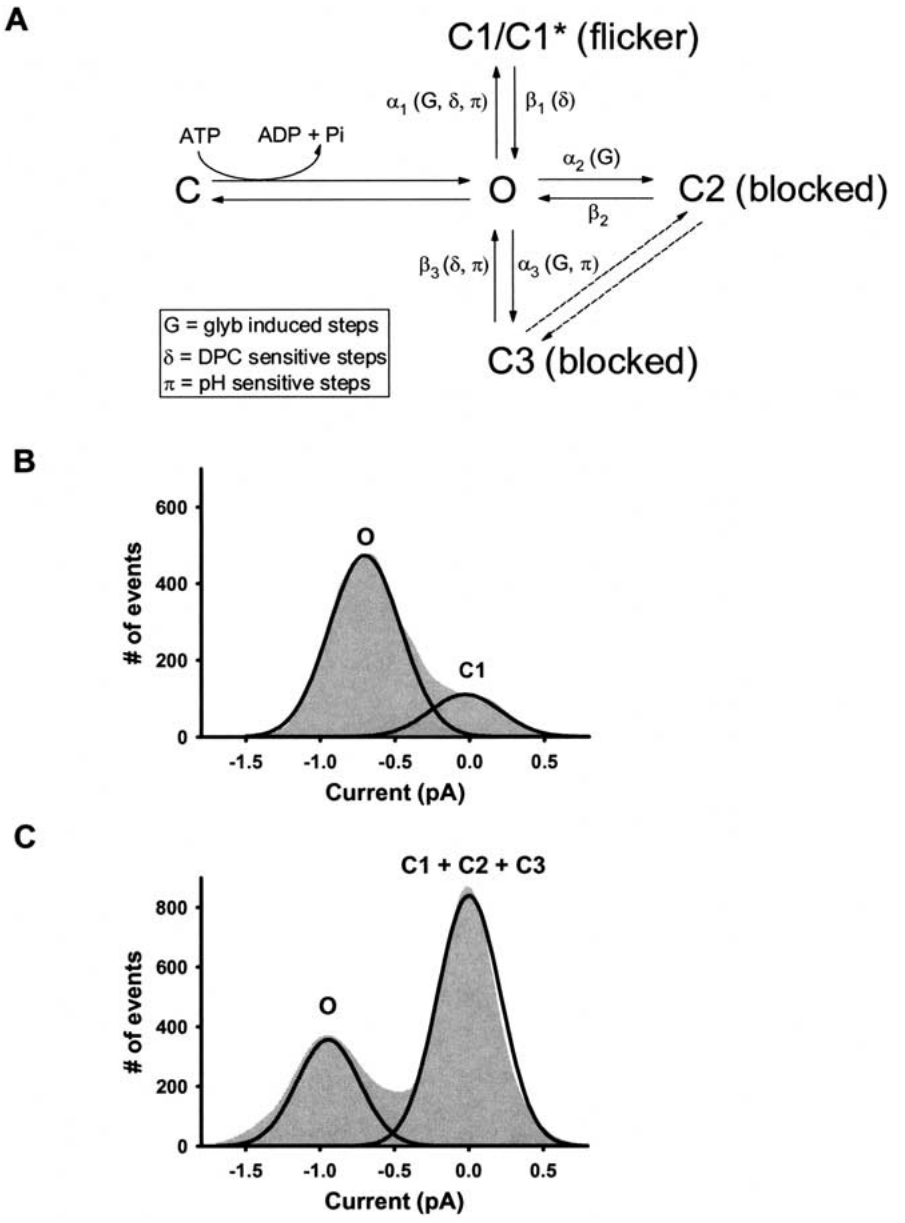

Fig. 9. (*A*) Model for the overall inhibition of single CFTR channels by glibenclamide. We assumed that the flickery closed state due to block by TES, the extremely brief closed state that may result from glibenclamide, and the DPC-induced closed state are the same; these closed states are kinetically indistinguishable. Steps that are sensitive to glibenclamide (G), DPC (δ), and cytosolic pH (π) are identified. The on-rate to the C1 state (α_1) is pH-dependent, while the on-rate to the C1* state is dependent upon glibenclamide, but is not sensitive to pH. The on-rates to C2 (α_2) and C3 (α_3) are glibenclamide-dependent, and α_3 is pH-dependent. Of the off-rates, only β_3 was pH-dependent The voltage dependence of block by glibenclamide predominantly arises from the voltage dependence of β_3 and α_3. (*B*) and (*C*) All-points amplitude histograms of bursts in the absence and presence of glibenclamide. (*B*) All-points amplitude histogram of the open burst depicted in Fig. 2*A* in the absence of exogenous blocker. From the areas under the closed and open states, the intraburst P_O was calculated to be 0.86 for this burst. (*C*) All-points amplitude histogram of an open burst in the presence of 25 μM glibenclamide depicted in Fig. 1*A*. From the areas under the closed and open states the intraburst P_O was calculated to be 0.44 for this burst. Solid lines show fits to a Gaussian function.

interaction with this site are only very weakly voltage-dependent. (Estimation of the physical distance through the voltage field using Woodhull [1973] analysis was not performed, since this approach assumes that the blocking molecule is in equilibrium with only a single binding site.) In contrast, the site corresponding to the C3 state appears to lie well within the voltage field of the membrane, as the kinetics of interaction with this site are strongly voltage-dependent. This is also supported by the finding that the binding site corresponding to the C3 state may lie close to the single binding site for DPC, which is predicted to experience approximately 41% of the voltage drop across the pore, measured from the cytoplasmic side (McCarty et al., 1993). The conclusion that these two glibenclamide binding sites are non-identical also is supported by the observation that interaction with the C3 site is pH-sensitive, while interaction with the C2 site is not.

Alternatively, the concentration-dependence of the glibenclamide-induced closed times may arise from alternative conformations of the drug within the pore. Since glibenclamide is a highly flexible molecule, there exists the possibility that the observed states reflect interactions of different parts of the drug with the walls of the channel pore; low affinity interactions of only one moiety of the drug molecule may result in the occupancy of the C2 state ($K_{d2} \cong 367$ μM), while interactions with both moieties result in higher affinity block and occupancy of the C3 state ($K_{d3} \cong 43$ μM). This would be consistent with the observed reduced frequency of this event, as the

likelihood of having the entire drug molecule bind should be lower than the likelihood of having part of the drug bind. Similarly, one would expect that interaction of more of the drug molecule with the pore would lead to a greater binding energy, and slower off-rate, as observed for the C3 state.

Glibenclamide binds to sites on the SUR1 sulfonylurea receptor with 1000-fold higher affinity than it does to CFTR; this is by a mechanism other than pore block because SUR1 does not form ion channels. The glibenclamide binding site on SUR1 is comprised of a high-affinity binding site for the sulfonylurea moiety of the drug, located in the C-terminal MSD containing helices 12–17, coupled to a binding site for the benzamido moiety, which is located between the first and second MSDs (Ashfield et al., 1999; Babenko, Ganzález & Bryan, 1999; Giblin, Quinn & Tinker, 2002); recent mutagenesis studies point to cytoplasmic loops rather than transmembrane domains themselves (Mikhailov, Mikhailova & Ashcroft, 2001). It seems possible that a similarly distributed binding pocket for glibenclamide may exist in CFTR. Consistent with this notion, Sheppard and coworkers recently showed that CFTR can be inhibited with low affinity by non-sulfonylurea hypoglycemic drugs, such as mitiglinide and meglitinide, which are related in structure to the benzamido moiety of glibenclamide (Cai, Lansdell & Sheppard, 1999). Mutagenesis studies will allow localization of the sites in CFTR that contribute to the C2 and C3 closed states, and will allow identification of portions of the CFTR molecule that interact with each moiety of the large glibenclamide molecule. Mutagenesis studies will also allow clarification of whether the C1* state reflects a true glibenclamide-induced closed state by assessing differential sensitivity of τ_{C1} and τ_{C1}* to pore-domain mutations. Indeed, Linsdell and colleague (Gupta & Linsdell, 2002) recently reported the effects of several point mutations upon block of CFTR by glibenclamide. The most significant change was seen with the T338A mutant in transmembrane domain 6, although this only reflected a two-fold decrease in affinity. The finding that no one-point mutation strongly affected affinity may be consistent with the presence of multiple binding sites, each of which contributes only a part of the energy of drug binding. Because those mutants were studied using macroscopic recording, it is impossible to determine whether the sites mutated may contribute to the C1*, C2, or C3 states described here.

It is important to note that our results differ significantly from those recently reported by Hwang and coworkers (Zhou et al., 2002). In that study, the behavior of mutant K1250A-CFTR was assayed with significant filtering of the single-channel records (100 Hz), resulting in loss of brief events. It is unclear whether this mutation, outside of the pore domain, might have any effect on block of the pore by glibenclamide; certainly, if glibenclamide binding is state-dependent, one would expect the results in K1250A-CFTR to differ substantially from those in *wt*-CFTR. Zhou and coworkers reported the appearance of a single glibenclamide-induced closed state with duration ~77 ms. Both the forward and, even more so, reverse rate constants were voltage-dependent (although, interestingly, not as voltage-dependent as block of macroscopic currents), but only the former was dependent upon drug concentration. However, filtering at 100 Hz, as used by Zhou et al., would preclude observation of brief states such as both C1* and C2 described here. Indeed, no records in the presence or absence of glibenclamide are shown at a high enough resolution to discern the 77 ms state or any other brief states, including that representing blockade by the "intrinsic blocker". In stark contrast, our analysis of intraburst behavior in weakly-filtered channel recordings of *wt*-CFTR indicates the presence of multiple interaction sites that differ in voltage-, concentration-, and pH-dependence.

Kinetically Distinct Intraburst States Differentiate Kinetic Models for Glibenclamide Action

Two previous models have been proposed to explain the effects of glibenclamide on single CFTR channels. Sheppard and Robinson (1997) proposed a linear scheme with a single blocked state; although these authors noted that $1/\tau_O$ has a non-zero value at zero added glibenclamide, they did not take this background block into account when estimating the on-rate for glibenclamide. The model proposed by Schultz and coworkers (Schultz et al., 1996) does provide for an additional state caused by the background flicker, but also included only one glibenclamide-induced closed state. To reduce the confounding effects of the glibenclamide-independent flicker, those authors chose to ignore all events less than 5 ms in duration, which would certainly eliminate detection of the C1* state and also would likely eliminate detection of the C2 state. Hence, neither of the previous studies detected a multi-exponential distribution of closed times in the presence of blocker. Furthermore, the inability to distinguish between open-blocked and open-closed events in these studies likely arises from the use of patches with relatively high channel activity and channel numbers.

Based on these previous studies and our current work, we constructed a model to explain the effects of glibenclamide within an open burst (Fig. 9). This model has five states: one open state (O) (a simplification, [Weinrich et al., 1999; Zeltwanger et al., 1999]), one interburst closed state (C), and three intraburst closed states C1/C1*, C2, and C3. The C1

state represents flickery block by the buffer, TES, and/or by DPC[1], while C1* represents either this state modified by the presence of glibenclamide or an indistinguishable glibenclamide-induced closed state of very brief duration. The C2 and C3 closed states represent the well-defined interactions of glibenclamide with sites within the pore, as evidenced by their dependence upon drug concentration and by their dependence upon the driving force for Cl^-.

One assumption of this model is that the three intraburst closed states may occur independently of each other (non-linear model). Because addition of glibenclamide results in a decrease in the open time it is not likely that glibenclamide induces new closed states that exclusively stem from the C1/C1* state. Because the duration of the drug-induced intraburst closed times increased with drug concentration, we propose that direct transitions between C2 and C3 states are possible (dashed lines in Fig. 9*A*).

From this model we can estimate the intraburst P_O at $V_M = -100$ mV and pH 7.3, using the following equation:

$$\text{intraburst } P_O = \frac{\tau_O}{\tau_O + m_1\tau_{C1/C1*} + m_2\tau_{C2} + m_3\tau_{C3}} \quad (2)$$

where τ_O, $\tau_{C1/C1}$*, τ_{C2}, and τ_{C3} are the intraburst time constants previously described, and m_1, m_2, and m_3 are the relative on-rates (α) to the respective closed states. Thus, $m_1 + m_2 + m_3 =$ unity. Using the rate constants for channels blocked by 25 μM glibenclamide (Tables 1 and 2), Eq. 2 predicts an intraburst P_O of 0.42.

This model was tested by determining the intraburst P_O using all-points histograms of multiple open-channel bursts. In the absence of exogenous blocker where m_2 and m_3 equal zero, this equation predicts an intraburst P_O of 0.93. This correlates well with our results, as evident in the all-points amplitude histogram from a burst in the absence of blocker (Fig. 9*B*). In the absence of glibenclamide, the mean intraburst P_O calculated from the relative areas of the peaks was 0.85 ± 0.3. In the presence of 25 μM glibenclamide, the peak representing the closed states is much larger (Fig. 9*C*). The intraburst P_O determined from multiple all-points amplitude histograms is 0.47 ± 0.03. This correlates relatively well with the P_O of 0.42 predicted by Eq. 2, suggesting that a model comprised of multiple binding sites may accurately describe the complexity of interactions between glibenclamide and CFTR.

[1]For simplicity's sake, this model assumes that the DPC-blocked state and the flickery blocked state (C1) are the same. Although other arylaminobenzoates have been shown to induce intraburst closed states that are separate from the flickery blocked state (McCarty et al., 1993; Zhang et al., 2000), only one intraburst closed time can be resolved in the presence of DPC alone.

Taken together, these data suggest that glibenclamide does not interact with the pore of the CFTR channel in the simple manner previously suggested. Instead, there appear to be multiple sites of interaction within the pore, leading to complex behavior of single CFTR channels in the presence of glibenclamide. These sites differ in pH- and voltage-dependence, suggesting that they may reflect different physical locations within the pore geometry.

This work was supported by the NSF (MCB-0077575), the American Heart Association (0140174 N) and the Cystic Fibrosis Foundation (MCCART00P0). N.A.M. is an Established Investigator of the American Heart Association. S.Z. was supported by an NIH post-doctoral training grant (DK-07656).

References

Aguilar-Bryan, L., Nichols, C.G., Wechsler, S.W., Clement, J.P. IV, Boyd, A.E. III, González, G., Herrera-Sosa, H., Nguy, K., Bryan, J., Nelson, D.A. 1995. Cloning of the β-cell high-affinity sulfonylurea receptor: a regulator of insulin secretion. *Science* **268:**423–426

Anderson, M.P., Rich, D.P., Gregory, R.J., Smith, A.E., Welsh, M.J. 1991. Generation of cAMP-stimulated chloride currents by expression of CFTR. *Science* **251:**679–682

Ashfield, R., Gribble, P.M., Ashcroft, S.J.H., Ashcroft, P.M. 1999. Identification of the high-affinity tolbutamide site on the SUR1 subunit of the K_{ATP} channel. *Diabetes* **48:**1341–1347

Babenko, A.P., González, G., Bryan, J. 1999. The tolbutamide site of SUR1 and a mechanism for its functional coupling to K_{ATP} channel closure. *FEBS Lett.* **459:**367–376

Bear, C.E., Li, C., Kartner, N., Bridges, R.J., Jensen, T.J., Ramjeesingh, M., Riordan, J.R. 1992. Purification and functional reconstitution of the cystic fibrosis transmembrane conductance regulator (CFTR). *Cell* **68:**809–818

Cai, Z., Lansdell, K.A., Sheppard, D.N. 1999. Inhibition of heterologously expressed cystic fibrosis transmembrane conductance regulator Cl^- channels by non-sulphonylurea hypoglycaemic agents. *Br. J. Pharmacol.* **128:**108–118

Cai, Z., Scott-Ward, T.S., Sheppard, D.N. 2003. Voltage-dependent gating of the cystic fibrosis transmembrane conductance regulator Cl^- channel. *J. Gen. Physiol.* **122:**605–620

Colquhoun, D., Hawkes, A.G. 1995. The principles of the stochastic interpretations of ion-channel mechanisms. *In:* Single-Channel Recording. B. Sakmann, E. Neher, editors. pp. 397–482, Plenum Press, New York.

Colquhoun, D., Sigworth, F.J. 1995. Fitting and statistical analysis of single-channel records. *In:* Single-Channel Recording. B. Sakmann, E. Neher, editors. pp. 483–587, Plenum Press, New York.

Cui, G., McCarty, N.A. 2003. Probing a new mechanism of glibenclamide interaction with CFTR: gating effects. *Biophys. J.* **84:**83a

Dawson, D.C., Liu, X., Zhang, Z.-R., McCarty, N.A. 2003. Anion conduction in CFTR: mechanisms and models. *In:* The CFTR Chloride Channel. K. Kirk, D.C., Dawson, editors. pp. 1–34, Landes Publishing, Georgetown, TX

Fischer, H., Machen, T.E. 1994. CFTR displays voltage dependence and two gating modes during stimulation. *J. Gen. Physiol.* **104:**541–566

Giblin, J.P., Quinn, K., Tinker, A. 2002. The cytoplasmic C-terminus of the sulfonylurea receptor is important for K_{ATP} channel function but is not key for complex assembly or trafficking. *Eur. J. Biochem.* **269:**5303–5313

Golstein, P.E., Boom, A., van Geffel, J., Jacobs, P., Masereel, B., Beauwens, R. 1999. P-glycoprotein inhibition by glibenclamide and related compounds. *Pfluegers. Arch.* **437:**652–660

Gupta, J., Linsdell, P. 2002. Point mutations in the pore region directly or indirectly affect glibenclamide block of the CFTR chloride channel. *Pfluegers. Arch.* **443:**739–747

Hanrahan, J.W., Tabcharani, J.A. 1990. Inhibition of an outwardly rectifying anion channel by HEPES and related buffers. *J. Membrane Biol.* **116:**65–77

Haws, C., Krouse, M.E., Xia, Y., Gruenert, D.C., Wine, JJ. 1992. CFTR channels in immortalized human airway cells. *Am. J. Physiol.* **263:**L692–L707

Ishihara, H., Welsh, M.J. 1997. Block by MOPS reveals a conformational change in the CFTR pore produced by ATP hydrolysis. *Am. J. Physiol.* **273:**C1278–C1289

Julien, M., Verrier, B., Cerutti, M., Chappe, V., Gola, M., Devauchelle, G., Becq, F. 1999. Cystic fibrosis transmembrane conductance regulator (CFTR) confers glibenclamide sensitivity to outwardly rectifying chloride channel (ORCC) in Hi-5 insect cells. *J. Membrane Biol.* **168:**229–239

Linsdell, P., Hanrahan, J.W. 1996. Disulphonic stilbene block of cystic fibrosis transmembrane conductance regulator Cl^- channels expressed in a mammalian cell line, and its regulation by a critical pore residue. *J. Physiol.* **496:**687–693

Luo, J., Pato, M.D., Riordan, J.R., Hanrahan, J.W. 1998. Differential regulation of single CFTR channels by PP2C, PP2A, and other phosphatases. *Am. J. Physiol.* **274:**C1397–1410

Mathews, C.J., Tabcharani, J.A., Chang, X.-B., Jensen, T.J., Riordan, J.R. Hanrahan, J.W. 1998. Dibasic protein kinase A sites regulate bursting rate and nucleotide sensitivity of the cystic fibrosis transmembrane conductance regulator. *J. Physiol.* **508:**365–377

McCarty, N.A. 2000. Permeation through the CFTR chloride channel. *J. Exp. Biol.* **203:**1947–1962

McCarty, N.A., McDonough, S., Cohen, B.N., Riordan, J.R., Davidson, N., Lester, HA. 1993. Voltage-dependent block of the cystic fibrosis transmembrane conductance regulator Cl^- channel by two closely related arylaminobenzoates. *J. Gen. Physiol.* **102:**1–23

McDonough, S., Davidson, N., Lester, H.A., McCarty, N.A. 1994. Novel pore-lining residues in CFTR that govern permeation and open-channel block. *Neuron.* **13:**623–634

McNicholas, CM., Guggino, W.B., Schwiebert, E.M., Hebert, S.C., Giebisch, G., Egan, M.E. 1996. Sensitivity of a renal K^+ channel (ROMK2) to the inhibitory sulfonylurea compound glibenclamide is enhanced by coexpression with the ATP-binding cassette transporter cystic fibrosis transmembrane regulator. *Proc. Natl. Acad. Sci. USA* **93:**8083–8088

Mehnert, H., Karg, E. 1969. Glibenclamid (HB419): ein neues orales Antidiabetikum der Sulfonycharnstoff-Reihe. *Deutsche Med. Wochen.* **94:**819–824

Mikhailov, M.V., Mikhailova, E.A., Ashcroft, S.J. 2001. Molecular structure of the glibenclamide binding site of the beta-cell K(ATP) channel. *FEBS Lett.* **499:**154–160

Neher, E., Steinbach, J.H. 1978. Local anaesthetics transiently block currents through single acetylcholine-receptor channels. *J. Physiol.* **277:**153–176

Ogden, D.C., Colquhoun, D. 1985. Ion channel block by acetylcholine, carbachol, and suberyldicholine at the frog neuromuscular junction. *Proc. Royal Soc. Lond.* **225:**329–355

Okuno, S., Inaba, M., Nishizawa, Y., Inoue, A., Mori, H. 1988. Effect of glyburide and tolbutamide on cAMP-dependent protein kinase activity in rat liver cytosol. *Diabetes* **37:**857–861

Quick, M.W., Naeve, J., Davidson, N., Lester, H.A. 1992. Incubation with horse serum increases viability and decreases background neurotransmitter uptake in *Xenopus* oocytes. *BioTechniques.* **13:**358–362

Rabe, A., Disser, J., Fromter, E. 1995. Cl^- channel inhibition by glibenclamide is not specific for the CFTR-type Cl^- channel. *Pfluegers Arch.* **429:**659–662

Riordan, J.R., Rommens, J.M., Kerem, B.-S., Alon, N., Rozmahel, R., Grzelczak, Z., Zielenski, J., Lok, S., Plavsic, N., Chou, J.-L., Drumm, M.L., lannuzzi, M.C., Collins, F.S., Tsui, L.-C. 1989. Identification of the cystic fibrosis gene: cloning and characterization of complementary DNA. *Science* **245:**1066–1072

Schultz, B.D., DeRoos, A.D.G., Venglarik, C.J., Singh, A.K., Frizzell, R.A., Bridges, R.J. 1996. Glibenclamide blockade of CFTR chloride channels. *Am. J. Physiol.* **271:**L192–L200

Schwiebert, E.M., Benos, D.J., Egan, M.E., Stutts, MJ., Guggino, W.B. 1999. CFTR is a conductance regulator as well as a chloride channel. *Physiol. Rev.* **79:**S145–S166

Sheppard, D.N., Robinson, K.A. 1997. Mechanism of glibenclamide inhibition of cystic fibrosis transmembrane conductance regulator Cl^- channels expressed in a murine cell line. *J. Physiol.* **503:**333–345

Sheppard, D.N., Welsh, M.J. 1992. Effect of ATP-sensitive K^+ channel regulators on cystic fibrosis transmembrane conductance regulator chloride currents. *J. Gen. Physiol.* **100:**573–592

Sturgess, N.C., Ashford, M.L.J., Cook, D.L., Hales, C.N. 1985. The sulphonylurea receptor may be an ATP-sensitive potassium channel. *Lancet.* **2:**474–475

Walsh, K.B., Long, K.J., Shen, X. 1999. Structural and ionic determinants of 5-nitro-2-(3-phenylpropylamino)-benzoic acid block of the CFTR chloride channel. *Br. J. Pharmacol.* **127:**369–376

Weinreich, F., Riordan, J.R., Nagel, G. 1999. Dual effects of ADP and adenylylimidodiphosphate on CFTR channel kinetics show binding to two different nucleotide binding sites. *J. Gen. Physiol.* **114:**55–70

Winter, M.C., Sheppard, D.N., Carson, M.R., Welsh, M.J. 1994. Effect of ATP concentration on CFTR Cl^- channels: a kinetic analysis of channel regulation. *Biophys. J.* **66:**1398–1403

Woodhull, A.M. 1973. Ionic blockage of sodium channels in nerve. *J. Gen. Physiol.* **61:**687–708

Yamazaki, J., Hume, J.R. 1997. Inhibitory effects of glibenclamide on cystic fibrosis transmembrane regulator, swelling-activated, and Ca^{2+} -activated Cl^- channels in mammalian cardiac myocytes. *Circ. Res.* **81:**101–109

Zeltwanger, S., Wang, F., Wang, G.-T., Gillis, K.D., Hwang, T.-C. 1999. Gating of cystic fibrosis transmembrane conductance regulator chloride channels by adenosine triphosphate hydrolysis: Quantitative analysis of a cyclic gating scheme. *J. Gen. Physiol.* **113:**541–554

Zeltwanger, S., Zhang, Z.-R., McCarty, N.A. 2000. Glibenclamide inhibits CFTR activity through interaction with multiple sites with varying affinities and pH-dependencies. *Biophys. J.* **78:**467A

Zhang, Z.-R., Zeltwanger, S., McCarty, N.A. 2000. Direct comparison of NPPB and DPC as probes of CFTR expressed in *Xenopus* oocytes. *J. Membrane Biol.* **175:**35–52

Zhang, Z.-R., Zeltwanger, S., Smith, S.S., Dawson, D.C., McCarty, N.A. 2002. Voltage-sensitive gating induced by a mutation in the fifth transmembrane domain of CFTR. *Am. J. Physiol.* **282:**L135–L145

Zhou, Z., Hu, S., Hwang, T.-C. 2001. Voltage-dependent flickery block of an open cystic fibrosis transmembrane conductance regulator (CFTR) channel pore. *J. Physiol.* **532:**435–448

Zhou, Z., Hu, S., Hwang, T.-C. 2002. Probing an open CFTR pore with organic anion blockers. *J. Gen. Physiol.* **120:**647–662

Zhu, T., Dahan, D., Evagelidis, A., Zheng, S., Luo, J., Hanrahan, J.W. 1999. Association of cystic fibrosis transmembrane conductance regulator and protein phosphatase 2C. *J. Biol. Chem.* **274:**29102–29107